Integration Filter for APS, DVL, IMU and Pressure Gauge for Underwater Vehicles

Fredrik Dukan *, **Asgeir J. Sørensen** *

* *Centre for Autonomous Marine Operations and Systems (AMOS), Department of Marine Technology, Norwegian University of Science and Technology, NTNU, NO-7491 Trondheim, Norway (e-mail: fredrik.dukan@ntnu.no, asgeir.sorensen@ntnu.no).*

Abstract: High-accuracy underwater navigation is important in order to automate motion control of remotely operated vehicles (ROVs). An observer that estimates the vehicle states (position, velocity, attitude and turn rates) is proposed for closed-loop control. Measurements from an acoustic positioning system (APS), a Doppler velocity log (DVL), an inertial measurement unit (IMU) and a pressure gauge (PG) are used in the proposed observer. The observer is divided into an attitude observer and a translational motion observer with interconnections. The attitude observer is an explicit complementary filter (ECF). Results from simulation are presented.

Keywords: ROV, Observer, State estimation, Integration filters, Underwater vehicles

1. INTRODUCTION

In order to automate motion control of underwater vehicles, the underwater navigation problem must be solved. One of the challenges is that GPS signals are not available underwater, and there is no global underwater positioning system today. Usually, an acoustic positioning system is used under water. However, the range is limited, and it requires installation of infrastructure or support from a surface vessel. In order to do closed-loop control of an underwater vehicle, such as an ROV, the 6-degrees of freedom (DOFs) states must be measured or estimated. This paper proposes a new observer which estimates the 6-DOF positions and velocities based on measurements from an acoustic positioning system, a DVL, an IMU and a pressure gauge. The goal is that the observer outputs an estimate with sufficient accuracy and smoothness for use in closed-loop control. The proposed observer is an adaption of the nonlinear observer presented in Grip et al. (2012a) and Grip et al. (2012b) which is an integration of Global navigation satellite systems (GNSS) and IMU measurements with gyro bias estimation.

The main contribution in the paper is the modification of the observer for body fixed velocities. A result is that the centripetal and translational acceleration can be calculated. This is used to improve the estimated attitude which again improves the estimated position and velocities from the integration filter. In addition, measurement equations for the ROV sensors are given, and simulation results are presented.

The observer is divided in two parts, one for attitude estimation based on the IMU measurements and one for translational motions. The attitude observer is from Mahony et al. (2008) and Mahony et al. (2009) and is termed an explicit complementary filter. It is formulated in terms of vectorial direction measurements that are compared to non-collinear reference vectors. A modification to this observer that also gives proof of stability for time-varying reference vectors is found in Grip et al. (2011). A summary of integration filters for IMU and GNSS is given in Fossen (2011). An introduction to strapdown inertial navigation technology is found in Titterton and Weston (2004). The notation used in this paper is adopted from Fossen (2011).

The paper is organized as follows. Section 2 gives a description of the measurements, sensors and the setup on an underwater vehicle. The measurement equations for the sensors are given in Section 3. The observer is presented in Section 4. Simulation results are given in Section 5, and a conclusion is found in Section 6.

2. SENSORS AND SETUP

4 different sensors units/packages are mounted on the underwater vehicle. These are a transponder (or transducer) for the APS, a DVL for measuring velocity w.r.t the water or the sea floor, an IMU that provides accelerations, turn rates and magnetic field measurements and a pressure gauge to measure the depth. A brief description and specifications of the sensors packages are given in the following. The sensors and their positions relative to the center of origin (CO) of the underwater vehicle is seen in Figure 1.

2.1 Transponder

The transponder sends and receives signals from an acoustic positioning system in order to determine the transponder position. Information about underwater acoustic positioning systems are found in Milne (1983) and Vickery (1998). The acoustic positioning system outputs the x, y and z position coordinates of the transponder. The APS update rate is about 1-3 Hz, dependent on water depth, in a typical ROV mission using a HiPAP system. The

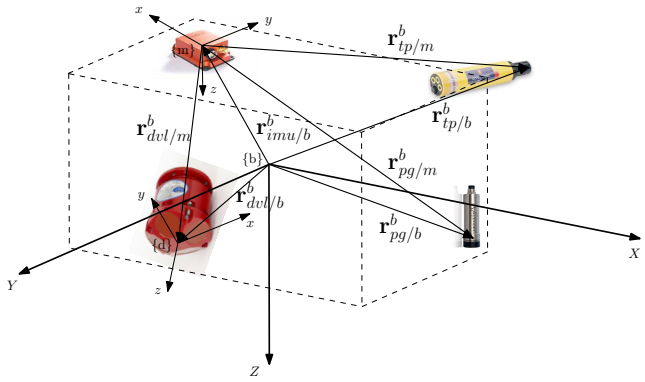

Fig. 1. Sensors and positions on the ROV.

standard deviation of the position error can be in order of meters for deep waters.

2.2 DVL

The DVL uses the Doppler shift in the echo of the acoustic signal sent from the 4 transducer heads to calculate the velocity vector of the DVL w.r.t the sea floor or the water column. Principals of operation are found in Gordon and Instruments (1996). The DVL outputs 3-DOF velocity measurements u, v, w in the DVL frame. A typical 600 kHz DVL has bottom track range from 0.7 m to 90 m with standard deviation of 0.3 cm/s at 1 m/s. Maximum ping rate is 7 Hz. As the DVL can be out of range, the observer must give estimates with sufficient quality for closed-loop control when the DVL is unavailable.

2.3 IMU

The observer proposed in the paper uses a so called 9-DOF IMU, which has 3 accelerometers, 3 gyroscopes and 3 magnetometers. This is used to measure the 3-DOF accelerations, turn rates and the magnetic field components. Recent advances in MEMS technology have resulted in high accuracy, small and inexpensive IMU units. These are well suited for use in smaller vehicles. A typical IMU has update rate of 100-1000 Hz, which is much faster than the APS and the DVL. Although the accuracy of the sensors is improving, there is still a problem with gyro drift. The magnetometers must be calibrated for soft and hard iron effects after the IMU is mounted on a vehicle.

2.4 Pressure Gauge

The pressure gauge is used to calculate the depth from a measured pressure. The accuracy of a high end sensor is typically $+/-0.01\%$ of full scale (FS) with resolution of 0.001% FS. Maximum update rate is 8 Hz. Note that the accuracy of the depth conversion also depends on the distribution of the density in the water column above the vehicle. The depth is also given by the acoustic positioning system, but the accuracy, resolution and update rate of the pressure gauge is superior to any APS. Hence, the depth measurements of the APS are not used in the observer.

2.5 Setup on Vehicle

Figure 1 shows the ROV fixed coordinate system $\{b\}$ and the outline of the ROV as a dashed box. The position of the sensor packages relative to the CO of the ROV fixed frame is given by the vectors $\boldsymbol{r}^b_{tp/b}$, $\boldsymbol{r}^b_{dvl/b}$, $\boldsymbol{r}^b_{imu/b}$ and $\boldsymbol{r}^b_{pg/b}$ for the transponder, DVL, IMU and pressure gauge respectively. The DVL and IMU outputs vectorial measurements in their own sensor frames $\{d\}$ and $\{m\}$. The orientation of $\{d\}$ and $\{m\}$ w.r.t $\{b\}$ is $\boldsymbol{\Theta}_{bd}$ and $\boldsymbol{\Theta}_{bm}$, respectively. As the observer (both parts) will be expressed in the IMU frame, the position of the other sensors relative to the IMU, in $\{m\}$, are needed. These are noted $\boldsymbol{r}^m_{tp/m}$, $\boldsymbol{r}^m_{dvl/m}$ and $\boldsymbol{r}^m_{pg/m}$ for the transponder, DVL, and pressure gauge respectively, see (1a), (1b) and (1c). The orientation vectors $\boldsymbol{\Theta}_{bd}$ and $\boldsymbol{\Theta}_{bm}$ are constant after the DVL and IMU are mounted on the vehicle. However, it is difficult to measure the orientations exactly. The alignment errors of the DVL and IMU can be a considerable source of error and will reduce the performance of the observer. A calibration should be done to obtain accurate values for $\boldsymbol{\Theta}_{bd}$ and $\boldsymbol{\Theta}_{bm}$. Ideally, the translational observer should include an alignment bias estimator. In practice, it is also difficult to measure the positions of the sensor packages exactly. This is another error source that will affect the performance of the observer.

$$\boldsymbol{r}^m_{tp/m} = \boldsymbol{R}^m_b(\boldsymbol{\Theta}_{bm})(\boldsymbol{r}^b_{tp/b} - \boldsymbol{r}^b_{imu/b}), \tag{1a}$$
$$\boldsymbol{r}^m_{dvl/m} = \boldsymbol{R}^m_b(\boldsymbol{\Theta}_{bm})(\boldsymbol{r}^b_{dvl/b} - \boldsymbol{r}^b_{imu/b}), \tag{1b}$$
$$\boldsymbol{r}^m_{pg/m} = \boldsymbol{R}^m_b(\boldsymbol{\Theta}_{bm})(\boldsymbol{r}^b_{pg/b} - \boldsymbol{r}^b_{imu/b}), \tag{1c}$$

where $\boldsymbol{R}^m_b(\boldsymbol{\Theta}_{bm}) \in \mathbb{R}^{3\times3}$ is the rotation matrix from $\{b\}$ to $\{m\}$.

3. MEASUREMENT EQUATIONS

The measurement equations for the IMU are given by (2a), (2b) and (2c) for the accelerometers, gyroscopes and magnetometers, respectively.

$$\begin{aligned}\boldsymbol{a}^m_{imu} &= \dot{\boldsymbol{v}}^m_{m/n} + \boldsymbol{\omega}^m_{m/n} \times \boldsymbol{v}^m_{m/n} - \boldsymbol{R}^m_n(\boldsymbol{\Theta}_{nm})\boldsymbol{g}^n \\ &\quad + \boldsymbol{b}^m_{acc} + \boldsymbol{w}^m_{acc}, \end{aligned}\tag{2a}$$
$$\boldsymbol{\omega}^m_{imu} = \boldsymbol{\omega}^m_{m/n} + \boldsymbol{b}^m_{gyro} + \boldsymbol{w}^m_{gyro}, \tag{2b}$$
$$\boldsymbol{m}^m_{imu} = \boldsymbol{R}^m_n(\boldsymbol{\Theta}_{nm})\boldsymbol{m}^n + \boldsymbol{b}^m_{mag} + \boldsymbol{w}^m_{mag}, \tag{2c}$$

where $\boldsymbol{a}^m_{imu} \in \mathbb{R}^3$ is the measured acceleration vector in $\{m\}$, $\dot{\boldsymbol{v}}^m_{m/n}$ is the true translational acceleration vector of the IMU. $\boldsymbol{\omega}^m_{m/n}$ is the true turn rate vector, $\boldsymbol{v}^m_{m/n}$ is the true velocity, and $\boldsymbol{\omega}^m_{m/n} \times \boldsymbol{v}^m_{m/n}$ is the centripetal acceleration of the IMU. $\boldsymbol{R}^m_n(\boldsymbol{\Theta}_{nm}) \in \mathbb{R}^{3\times3}$ is the rotation matrix from $\{n\}$ to $\{m\}$, and $\boldsymbol{\Theta}_{nm}$ is the attitude of the IMU. $\boldsymbol{g}^n$ is the gravity acceleration vector, $\boldsymbol{b}^m_{acc}$ is the accelerometer bias vector, and $\boldsymbol{w}^m_{acc}$ is the accelerometer noise vector.

$\boldsymbol{\omega}^m_{imu} \in \mathbb{R}^3$ is the measured turn rate vector of the IMU, $\boldsymbol{b}^m_{gyro}$ is the gyroscope bias vector and $\boldsymbol{w}^m_{gyro}$ is the gyroscope noise vector.

$\boldsymbol{m}^m_{imu} \in \mathbb{R}^3$ is the measured magnetic field vector in $\{m\}$, $\boldsymbol{m}^n$ is the true magnetic field vector in $\{n\}$. $\boldsymbol{b}^m_{mag}$ is the magnetometer bias vector and $\boldsymbol{w}^m_{mag}$ is the magnetometer noise vector.

The measurement equations for the transponder and DVL are given by (3a) and (3b), respectively.

$$\boldsymbol{p}^n_{tp/n} = \boldsymbol{p}^n_{m/n} + \boldsymbol{R}^n_m(\boldsymbol{\Theta}_{nm})\boldsymbol{r}^m_{tp/m} + \boldsymbol{w}^n_{tp}, \tag{3a}$$

$$\boldsymbol{v}^d_{d/n} = \boldsymbol{R}^d_b(\boldsymbol{\Theta}_{bd})\boldsymbol{R}^b_m(\boldsymbol{\Theta}_{bm})(\boldsymbol{v}^m_{m/n} + \boldsymbol{\omega}^m_{m/n} \times \boldsymbol{r}^m_{dvl/m}) + \boldsymbol{w}^d_{dvl}, \tag{3b}$$

where $\boldsymbol{p}^n_{tp/n} \in \mathbb{R}^3$ is the measured transponder position in $\{n\}$, $\boldsymbol{p}^n_{m/n}$ is the true IMU position and $\boldsymbol{w}^n_{tp}$ is the APS noise. $\boldsymbol{v}^d_{d/n} \in \mathbb{R}^3$ is the measured velocity in $\{d\}$, and $\boldsymbol{w}^d_{dvl}$ is the DVL noise.

The measurement equations for the pressure gauge is given by (4a) and (4b).

$$p_{pg} = p_{atm} + \rho g z^n_{pg/n} + w_{pg}, \tag{4a}$$

$$z^n_{pg/n} = z^n_{m/n} + [0\ 0\ 1]\boldsymbol{R}^n_b(\boldsymbol{\Theta})\boldsymbol{r}^m_{pg/m}, \tag{4b}$$

where $p_{pg} \in \mathbb{R}$ is the measured pressure, p_{atm} is the atmospheric pressure at the surface, ρ is the water density, g is the acceleration of gravity, $z^n_{pg/n}$ is the depth of the pressure gauge, and w_{pg} is the PG noise. $z^n_{m/n}$ is the depth of the IMU. Eq. (4a) is only valid for constant water density throughout the water column. For real implementations, more refined measurement equations for converting pressure to depth should be used, e.g. the depth conversion formula in Fofonoff and Millard (1983).

4. OBSERVER

The proposed observer estimates the 6-DOF position and velocity vector of the ROV. The dynamics of the position, velocity and attitude is given by (5a), (5b) and (5c).

$$\dot{\boldsymbol{p}}^n_{m/n} = \boldsymbol{R}^n_m(\boldsymbol{\Theta}_{nm})\boldsymbol{v}^m_{m/n}, \tag{5a}$$

$$\dot{\boldsymbol{v}}^m_{m/n} = \boldsymbol{a}^m_{m/n} - \boldsymbol{\omega}^m_{m/n} \times \boldsymbol{v}^m_{m/n} + \boldsymbol{R}^m_n(\boldsymbol{\Theta}_{nm})\boldsymbol{g}^n, \tag{5b}$$

$$\dot{\boldsymbol{R}}^n_m = \boldsymbol{R}^n_m \boldsymbol{S}(\boldsymbol{\omega}^m_{m/n}), \tag{5c}$$

where $\boldsymbol{a}^m_{m/n}$ is the acceleration felt by the accelerometer, and $\boldsymbol{S}(\cdot)$ is the cross product operator. In this paper it is assumed that $\{n\}$ is an inertial reference frame. For improved performance in actual implementations, (5b) should be expressed with respect to the Earth-centered inertial (ECI) frame, $\{i\}$.

First, all measurements are transformed to the IMU frame where the observer is expressed. The observer is divided in two stages. One for the translational motions and one for attitude. The two observer stages are interconnected as illustrated in Figure 2. Both the translational and attitude observer run at the same high frequency, but not higher than the IMU frequency. However, the gains corresponding to a sensor measurement are zero when the measurement is unavailable.

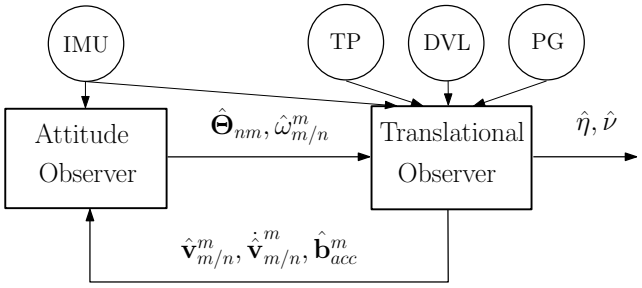

Fig. 2. Interconnection between the attitude and translational observers.

Finally, the estimated states of the IMU are transformed to the CO of the ROV to give $\hat{\boldsymbol{\eta}}$ and $\hat{\boldsymbol{\nu}}$ which are the estimated generalized 6-DOF position and velocity vectors of the ROV.

The transponder, pressure gauge and DVL measurements are transformed to the IMU frame and position in (6a), (6b) and (6c), respectively. Note that in (6b) the depth in the position vector of the IMU is replaced by the PG measurements as this is superior to the APS depth from (6a).

$$\boldsymbol{p}^n_{m/n} = \boldsymbol{p}^n_{tp/n} - \boldsymbol{R}^n_m(\hat{\boldsymbol{\Theta}}_{nm})\boldsymbol{r}^m_{tp/m}, \tag{6a}$$

$$\boldsymbol{p}^n_{m/n}(3) = z^n_{pg/n} - [0\ 0\ 1]\boldsymbol{R}^n_m(\hat{\boldsymbol{\Theta}}_{nm})\boldsymbol{r}^m_{pg/m}, \tag{6b}$$

$$\boldsymbol{v}^m_{m/n} = \boldsymbol{R}^m_b(\boldsymbol{\Theta}_{bm})\boldsymbol{R}^b_d(\boldsymbol{\Theta}_{bd})\boldsymbol{v}^d_{d/n} - \hat{\boldsymbol{\omega}}^m_{m/n} \times \boldsymbol{r}^m_{dvl/m}, \tag{6c}$$

where $\hat{\boldsymbol{\Theta}}_{nm}$ and $\hat{\boldsymbol{\omega}}^m_{m/n}$ are the estimated attitude and turn rate of the IMU.

4.1 Translational Observer

By copying (5a) and (5b) and adding injection terms and a bias estimator for the accelerometer, the following translational observer is proposed.

$$\dot{\hat{\boldsymbol{p}}}^n_{m/n} = \boldsymbol{R}^n_m(\hat{\boldsymbol{\Theta}}_{nm})(\hat{\boldsymbol{v}}^m_{m/n} + \boldsymbol{K}_{21}\tilde{\boldsymbol{y}}_2) + \boldsymbol{K}_{11}\tilde{\boldsymbol{y}}_1, \tag{7a}$$

$$\dot{\hat{\boldsymbol{v}}}^m_{m/n} = \boldsymbol{a}^m_{imu} - \hat{\boldsymbol{\omega}}^m_{m/n} \times \hat{\boldsymbol{v}}^m_{m/n} - \hat{\boldsymbol{b}}^m_{acc} + \boldsymbol{R}^m_n(\hat{\boldsymbol{\Theta}}_{nm})(\boldsymbol{g}^n + \boldsymbol{K}_{12}\tilde{\boldsymbol{y}}_1) + \boldsymbol{K}_{22}\tilde{\boldsymbol{y}}_2, \tag{7b}$$

$$\dot{\hat{\boldsymbol{b}}}^m_{acc} = -\boldsymbol{K}_{13}\boldsymbol{R}^m_n(\hat{\boldsymbol{\Theta}}_{nm})\tilde{\boldsymbol{y}}_1 - \boldsymbol{K}_{23}\tilde{\boldsymbol{y}}_2, \tag{7c}$$

where $\boldsymbol{K}_{11}$, $\boldsymbol{K}_{21}$, $\boldsymbol{K}_{12}$, $\boldsymbol{K}_{22}$, $\boldsymbol{K}_{13}$ and $\boldsymbol{K}_{23} \in \mathbb{R}^{3\times3}$ are gain matrices. The estimation errors used in the injection terms are given by (8a) and (8b) for translational position and velocity respectively.

$$\tilde{\boldsymbol{y}}_1 = \boldsymbol{p}^n_{m/n} - \hat{\boldsymbol{p}}^n_{m/n}, \tag{8a}$$

$$\tilde{\boldsymbol{y}}_2 = \boldsymbol{v}^m_{m/n} - \hat{\boldsymbol{v}}^m_{m/n}. \tag{8b}$$

The observer gain matrices are chosen to have the structure in (9) as suggested in Fossen (2011).

$$\boldsymbol{K}_i = \text{diag}\{k_i, k_i, l_i\}, \quad i = 1, 2, 3. \tag{9}$$

where surge and sway have the same gains $k_i > 0$ and heave is tuned by $l_i > 0$.

Note that the velocity and position estimates in the translational observer can drift rapidly in case of drop-out of both velocity and position measurements. Even a small error in the attitude estimation will yield quick drift of the velocity estimate due to the rotation matrix in (7b).

4.2 Attitude Observer

The attitude observer is termed an explicit complementary filter. The main idea is to measure the acceleration and magnetic field vectors in $\{m\}$ and compare these to reference vectors in $\{n\}$ after transformation to $\{m\}$ by using the estimated attitude. Normalized vectors are used for comparison. The gyroscopes provide complementary measurements.

IMU vectors The normalized acceleration and magnetic field vectors in $\{m\}$ are given by (10) as,

$$\boldsymbol{v}_1^m = \frac{\bar{\boldsymbol{a}}_{imu}^m}{||\bar{\boldsymbol{a}}_{imu}^m||}, \quad \boldsymbol{v}_2^m = \frac{\boldsymbol{m}_{imu}^m}{||\boldsymbol{m}_{imu}^m||}. \tag{10}$$

$$\bar{\boldsymbol{a}}_{imu}^m = \boldsymbol{a}_{imu}^m - \hat{\boldsymbol{\omega}}_{m/n}^m \times \hat{\boldsymbol{v}}_{m/n}^m - \dot{\hat{\boldsymbol{v}}}_{m/n}^m - \hat{\boldsymbol{b}}_{acc}^m. \tag{11}$$

where $\bar{\boldsymbol{a}}_{imu}^m$ as in (11) is the measured acceleration vector adjusted for centripetal and translational acceleration and accelerometer bias as estimated in the translational observer. Ideally the modified acceleration should be $\bar{\boldsymbol{a}}_{imu}^m = \boldsymbol{R}_n^m(\boldsymbol{\Theta}_{nm})\boldsymbol{g}^n$. This feedback to the attitude observer is seen in Figure 2. In a stand alone IMU attitude observer, the vector $\boldsymbol{v}_1^m$ is calculated from the measured accelerations $\boldsymbol{a}_{imu}^m$. Then it is not possible to separate measured accelerations due to attitude from centripetal and translational accelerations. However, a stand alone attitude observer can still give good results if the mean acceleration is zero and these acceleration phases have short duration. This works because the filter is complemented by gyroscope measurements as well.

Reference vectors The reference vectors in $\{n\}$ for acceleration and magnetic field measurements are given by (12). $\boldsymbol{v}_{01}^n$ is independent of latitude in the local NED frame by default. $\boldsymbol{v}_{02}^n$ varies with latitude because of the angle of inclination of the Earth's magnetic field increases with latitude.

$$\boldsymbol{v}_{01}^n = \frac{\boldsymbol{g}^n}{||\boldsymbol{g}^n||} = \begin{bmatrix} 0 \\ 0 \\ -1 \end{bmatrix}, \quad \boldsymbol{v}_{02}^n = \frac{\boldsymbol{m}^n}{||\boldsymbol{m}^n||}. \tag{12}$$

The reference vectors in (12) must be transformed to $\{m\}$ in order to compare them with the measurement vectors in (10). The transformation is given by (13) for the attitude expressed in quaternions. Note that $\hat{\boldsymbol{q}} = \boldsymbol{q}$ when $\hat{\boldsymbol{v}}_i^m = \boldsymbol{v}_i^m$.

$$\hat{\boldsymbol{v}}_1^m = \boldsymbol{R}_n^m(\hat{\boldsymbol{q}})\boldsymbol{v}_{01}^n, \quad \hat{\boldsymbol{v}}_2^m = \boldsymbol{R}_n^m(\hat{\boldsymbol{q}})\boldsymbol{v}_{02}^n, \tag{13}$$

where $\hat{\boldsymbol{q}}$ is estimated by the explicit complementary filter as shown next.

Explicit Complementary Filter The explicit complementary filter equations are given by (14a), (14b) and (14c). The equations are taken from Fossen (2011).

$$\boldsymbol{\omega}_{mes}^m = -\text{vex}\left(\sum_{i=1}^{2} \frac{k_i}{2}\left(\boldsymbol{v}_i^m(\hat{\boldsymbol{v}}_i^m)^T - \hat{\boldsymbol{v}}_i^m(\boldsymbol{v}_i^m)^T\right)\right) \tag{14a}$$

$$\dot{\hat{\boldsymbol{q}}} = \boldsymbol{T}_q(\hat{\boldsymbol{q}})\left[\boldsymbol{\omega}_{imu}^m - \hat{\boldsymbol{b}}_{gyro}^m + \boldsymbol{K}_p\boldsymbol{\omega}_{mes}^m\right], \tag{14b}$$

$$\dot{\hat{\boldsymbol{b}}}_{gyro}^m = -\frac{1}{2}\boldsymbol{K}_i\boldsymbol{\omega}_{mes}^m, \tag{14c}$$

where $\boldsymbol{\omega}_{mes}^m \in \mathbb{R}^3$ is the injection term. k_i is a gain to weight acceleration and magnetic field vectors. $\boldsymbol{T}_q(\hat{\boldsymbol{q}})$ is the angular velocity transformation from euler angle rates to quaternion rates. $\boldsymbol{K}_p \in \mathbb{R}^{3\times3}$ is an observer gain matrix and $\boldsymbol{K}_i \in \mathbb{R}^{3\times3}$ is the gyro bias estimation gain matrix. $\boldsymbol{K}_p$ and $\boldsymbol{K}_i$ are set to be diagonal matrices. The vex operator is the inverse of the cross product operator $\boldsymbol{S}(\cdot)$. The output of the ECF is the estimated attitude vector of the IMU, $\hat{\boldsymbol{q}}$, which can be transformed to euler angles to obtain $\hat{\boldsymbol{\Theta}}_{nm}$.

4.3 Transformation to Vehicle Frame

Both the translational and attitude observer are expressed in $\{m\}$. The estimated states must be transformed to the vehicle frame and CO before use in the vehicle control system. This transformation is given by (15a)-(15d).

$$\boldsymbol{\Theta}_{nb} = \boldsymbol{\Theta}_{nm} - \boldsymbol{\Theta}_{bm}, \tag{15a}$$

$$\boldsymbol{p}_{b/n}^n = \boldsymbol{p}_{m/n}^n - \boldsymbol{R}_b^n(\boldsymbol{\Theta}_{nb})\boldsymbol{r}_{imu/b}^b, \tag{15b}$$

$$\boldsymbol{\omega}_{b/n}^b = \boldsymbol{T}_\Theta(\boldsymbol{\Theta}_{bm})\boldsymbol{\omega}_{m/n}^m, \tag{15c}$$

$$\boldsymbol{v}_{b/n}^b = \boldsymbol{R}_m^b(\boldsymbol{\Theta}_{bm})\boldsymbol{v}_{m/n}^m - \boldsymbol{\omega}_{b/n}^b \times \boldsymbol{r}_{imu/b}^b, \tag{15d}$$

where $\boldsymbol{p}_{b/n}^n$ is the position of the CO in $\{n\}$, $\boldsymbol{\Theta}_{nb}$ is the vehicle attitude, $\boldsymbol{v}_{b/n}^b$ is the vehicle velocity in $\{b\}$ and $\boldsymbol{\omega}_{b/n}^b$ is the vehicle turn rate vector. $\boldsymbol{T}_\Theta$ is the transformation matrix from turn rates in $\{m\}$ to $\{b\}$.

The final result of the integration filter is the estimated generalized coordinates $\hat{\boldsymbol{\eta}}$ and $\hat{\boldsymbol{\nu}}$ as seen in (16).

$$\hat{\boldsymbol{\eta}} = \begin{bmatrix} \hat{\boldsymbol{p}}_{b/n}^n \\ \hat{\boldsymbol{\Theta}}_{nb} \end{bmatrix}, \quad \hat{\boldsymbol{\nu}} = \begin{bmatrix} \hat{\boldsymbol{v}}_{b/n}^b \\ \hat{\boldsymbol{\omega}}_{b/n}^b \end{bmatrix}. \tag{16}$$

5. SIMULATION

Results from simulation are shown in the following. The output of the vehicle simulation model is the generalized state vectors $\boldsymbol{\eta}$, $\boldsymbol{\nu}$ and $\dot{\boldsymbol{\nu}}$. From the state vectors, the sensor measurements are obtained from (17a), (17b) and (17c) for the transponder, pressure gauge and DVL, respectively.

$$\boldsymbol{p}_{tp}^n = \boldsymbol{p}_{b/n}^n + \boldsymbol{R}_b^n(\boldsymbol{\Theta}_{nb})\boldsymbol{r}_{tp/b}^b, \tag{17a}$$

$$z_{pg/n}^n = [0\ 0\ 1](\boldsymbol{p}_{b/n}^n + \boldsymbol{R}_b^n(\boldsymbol{\Theta}_{nb})\boldsymbol{r}_{pg/b}^b), \tag{17b}$$

$$\boldsymbol{v}_{d/n}^d = \boldsymbol{R}_b^d(\boldsymbol{\Theta}_{bd})(\boldsymbol{v}_{b/n}^b + \boldsymbol{\omega}_{b/n}^b \times \boldsymbol{r}_{dvl/b}^b). \tag{17c}$$

The IMU measurements are obtained from (18a), (18b) and (18c).

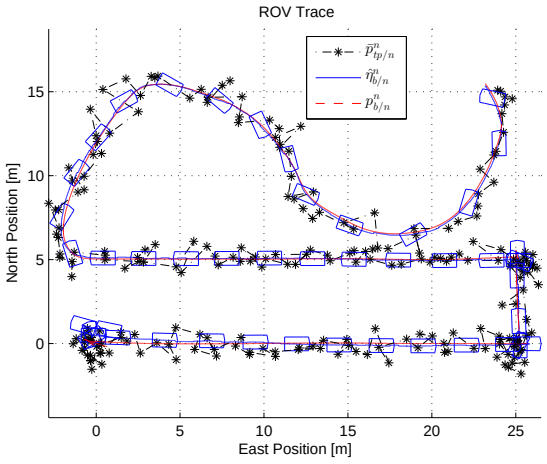

Fig. 3. ROV trace and outline, case 1.

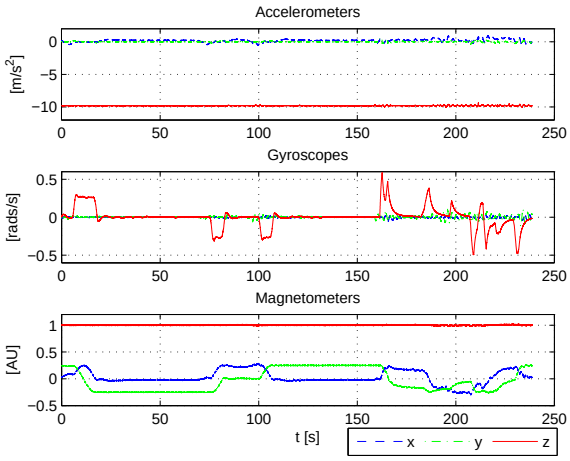

Fig. 4. IMU data.

$$\boldsymbol{a}^m_{imu} = \boldsymbol{R}^m_b(\boldsymbol{\Theta}_{bm})(\dot{\boldsymbol{v}}^b_{b/n} + \boldsymbol{\omega}^b_{b/n} \times \boldsymbol{v}^b_{b/n} + \dot{\boldsymbol{\omega}}^b_{b/n} \times \boldsymbol{r}^b_{imu/b} + \boldsymbol{\omega}^b_{b/n} \times (\boldsymbol{\omega}^b_{b/n} \times \boldsymbol{r}^b_{imu/b}) - \boldsymbol{R}^b_n(\boldsymbol{\Theta}_{nb})\boldsymbol{g}^n), \quad (18a)$$

$$\boldsymbol{\omega}^m_{imu} = \boldsymbol{T}^{-1}_{\Theta}(\boldsymbol{\Theta}_{bm})\boldsymbol{\omega}^b_{b/n}, \quad (18b)$$

$$\boldsymbol{m}^m_{imu} = \boldsymbol{R}^m_b(\boldsymbol{\Theta}_{bm})\boldsymbol{R}^b_n(\boldsymbol{\Theta}_{nb})\boldsymbol{m}^n. \quad (18c)$$

The DVL and transponder are mounted on the centerline at the stern and the IMU on the port side of the bow. The DVL is oriented 45 degrees in yaw w.r.t the ROV and the IMU is aligned with the ROV. More exactly, in meters,

$$\boldsymbol{r}^b_{tp/b} = [-0.75, 0, -0.45]^T, \quad \boldsymbol{r}^b_{dvl/b} = [-0.75, 0, 0.25]^T,$$
$$\boldsymbol{r}^b_{imu/b} = [0.79, -0.39, -0.35]^T \text{ and } \boldsymbol{r}^b_{pg/b} = [0, 0, 0.2]^T.$$

In the simulation case, the ROV first moves 2 legs at 0.5 m/s in a lawnmower pattern before it does a s-turn under joystick control. The maneuver is seen in Figure 3 which shows the transponder measurements (black stars), ROV estimated (blue) and true (red) traces and snapshots of its outline at the estimated position every 5^{th} second. It is seen that the position estimates are smooth and accurate. The IMU data are shown in Figure 4. The transponder measurements are updated at 1 Hz, the DVL at 5 Hz, the PG at 8 Hz and the IMU at 100 Hz. Noise is added to all measurements with standard deviation of 0.5 m for the TP, 0.003 m/s for the DVL, 0.0001 bar for the PG, 0.007 m/s^2 for the accelerometer, 0.0012 rads/s for the gyroscope and 0.0035 AU for the magnetometer. A bias is added to the simulated gyroscope measurements, $\boldsymbol{b}^m_{gyro} = [-1.4, 1.9, 0.9]^T \cdot 10^{-3}$ rads/s.

The observer gains for the translational observer are $\boldsymbol{K}_{11} = \text{diag}\{5, 5, 0.1\}$, $\boldsymbol{K}_{12} = 0.1\boldsymbol{I}$, $\boldsymbol{K}_{21} = 5\boldsymbol{I}$, $\boldsymbol{K}_{22} = 20\boldsymbol{I}$. $\boldsymbol{K}_{13} = 0\boldsymbol{I}$ and $\boldsymbol{K}_{23} = 0\boldsymbol{I}$ as the simulated accelerometers are bias free. The attitude observer gains are set to $k_i = 1,\ i = 1, 2$, $\boldsymbol{K}_p = \text{diag}\{1, 1, 10\}$ and $\boldsymbol{K}_i = 0.3\boldsymbol{I}$. At each iteration, the attitude observer is run first to provide an estimated attitude for the translational observer.

The case is run two times without and with feedback between the translational and attitude observer, see Figure 2. I.e. in case 0, without feedback, (11) is reduced to $\bar{\boldsymbol{a}}^m_{imu} = \boldsymbol{a}^m_{imu}$. Eq. (11) is used in case 1, with feedback. The interconnection enhances the performance of both observers as shown in Figure 5, 6 and 7 where case 0 is blue and case 1 is red.

Figure 5 shows the estimated attitude errors. Note the superior performance of case 1 during turns of the ROV. The IMU is mounted at a corner of the ROV so that it experiences centripetal accelerations also during pure turns of the ROV. Without the observer feedback, the attitude observer sees this as a roll and pitch motion as it can not separate the centripetal and translational acceleration from the acceleration of gravity. This causes an erroneous attitude which is used in the translational observer to integrate the accelerometer measurements to obtain estimated velocities. Hence errors propagate to the estimated velocity and position as well in case 0.

Figure 6 shows the estimated velocity error $\tilde{\boldsymbol{y}}_2$ using the true value of $\boldsymbol{v}^m_{m/n}$. The measured value of $\boldsymbol{v}^m_{m/n}$ is used in the observer. It is clear that the velocity error during periods of proper acceleration is affected by the attitude error in case 0.

Figure 7 shows the estimated position error $\tilde{\boldsymbol{y}}_1$. Again, the plotted errors are calculated from the true values and the measured values are used in the observer. The observer is initialized with the measured position. Note that the estimation error is smallest for case 1 as the velocity errors from case 0 propagate to the estimated position.

The estimated gyro bias is seen in Figure 8. The estimated bias starts at 0 and converges rapidly to the true values. A trick is used to accelerate the convergence of the bias estimates. At start up, the gain $\boldsymbol{K}_i = 2.2\boldsymbol{I}$ and decays exponentially to the final gain $\boldsymbol{K}_i = 0.3\boldsymbol{I}$ in 30 seconds.

6. CONCLUSION

The proposed observer gave promising results in simulation with realistic measurement data in terms of update rates and noise. The proposed interaction (acceleration feedback) between the translational and attitude observer greatly improved the performance of both observers. However, formal stability proofs for both observers with the proposed feedback/interaction are needed.

Drop-out of both position and velocity measurements for longer time periods is a problem. The translational

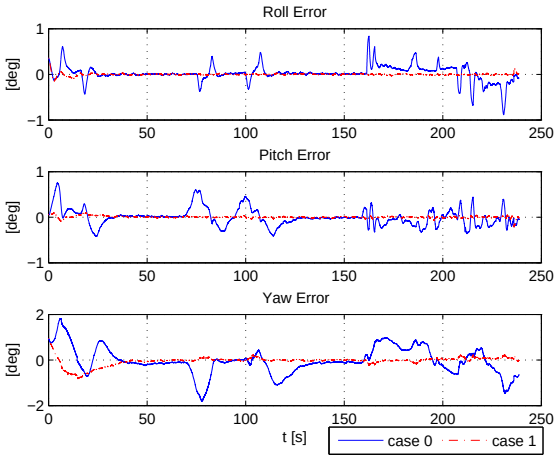

Fig. 5. Attitude errors, case 0 (blue) and 1 (red).

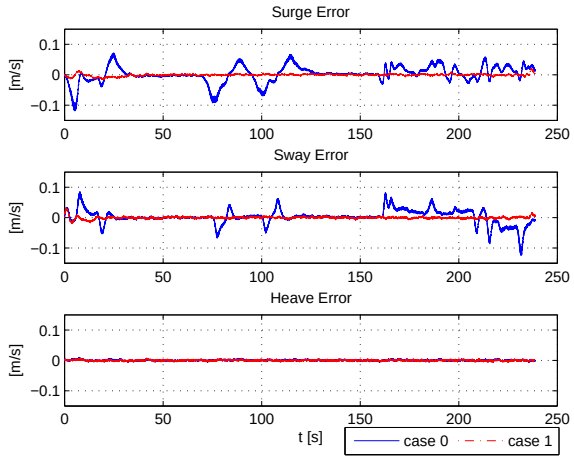

Fig. 6. Velocity errors, case 0 (blue) and 1 (red).

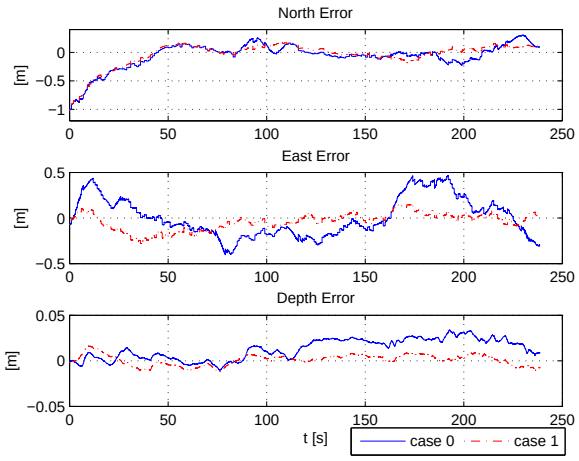

Fig. 7. Position errors, case 0 (blue) and 1 (red).

observer is not well suited for dead-reckoning as even the smallest error in attitude will cause the velocity estimate to drift quickly.

It is concluded that this type of observer is suitable for smaller underwater vehicles as it relies on small and inexpensive sensors and it does not depend on a dynamic

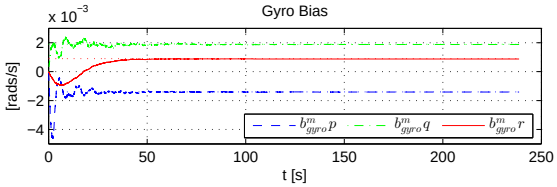

Fig. 8. Gyro bias estimation, case 1.

model of the vehicle. The latter is important as the hydrodynamics of underwater vehicles and forces from manipulation work may be very complex and difficult to model.

ACKNOWLEDGEMENTS

This work has been carried out at the Centre for Autonomous Marine Operations and Systems (AMOS). The Norwegian Research Council is acknowledged as the main sponsor of AMOS.

REFERENCES

Fofonoff, N.P. and Millard, R.C. (1983). Algorithms for computation of fundamental properties of seawater.

Fossen, T.I. (2011). *Handbook of Marine Craft Hydrodynamics and Motion Control*. John Wiley and Sons Ltd.

Gordon, R.L. and Instruments, R. (1996). Principles of operation a practical primer. *RD Instruments, San Diego*.

Grip, H.F., Fossen, T.I., Johansen, T.A., and Saberi, A. (2011). Attitude estimation based on time-varying reference vectors with biased gyro and vector measurements. *Proc. IFAC World Congr., Milan, Italy*, 8497–8502.

Grip, H.F., Fossen, T.I., Johansen, T.A., and Saberi, A. (2012a). Attitude estimation using biased gyro and vector measurements with time-varying reference vectors. *Automatic Control, IEEE Transactions on*, 57(5), 1332–1338.

Grip, H.F., Fossen, T.I., Johansen, T.A., and Saberi, A. (2012b). A nonlinear observer for integration of gnss and imu measurements with gyro bias estimation. In *American Control Conference (ACC), 2012*, 4607–4612. IEEE.

Mahony, R., Hamel, T., Trumpf, J., and Lageman, C. (2009). Nonlinear attitude observers on so (3) for complementary and compatible measurements: A theoretical study. In *Decision and Control, 2009 held jointly with the 2009 28th Chinese Control Conference. CDC/CCC 2009. Proceedings of the 48th IEEE Conference on*, 6407–6412. IEEE.

Mahony, R., Hamel, T., and Pflimlin, J.M. (2008). Nonlinear complementary filters on the special orthogonal group. *Automatic Control, IEEE Transactions on*, 53(5), 1203–1218.

Milne, P.H. (1983). Underwater acoustic positioning systems.

Titterton, D. and Weston, J. (2004). Strapdown inertial navigation technology. 2-nd edition. *The Institution of Electronical Engineers, Reston USA*.

Vickery, K. (1998). Acoustic positioning systems. a practical overview of current systems. In *Autonomous Underwater Vehicles, 1998. AUV'98. Proceedings Of The 1998 Workshop on*, 5–17. IEEE.